

# CALIBRATION AND INTERPRETATION OF ACOUSTIC BACKSCATTER MEASUREMENTS OF SUSPENDED SEDIMENT CONCENTRATION PROFILES IN SYDNEY HARBOUR

L.J. Hamilton

Aeronautical and Maritime Research Laboratory,  
Defence Science & Technology Organisation (DSTO),  
P.O. Box 44, Pyrmont, New South Wales 2009, Australia

**ABSTRACT** An 0.5 MHz acoustic backscatter (ABS) device developed and manufactured by Shanghai Acoustics Laboratory was used to infer vertical profiles of suspended sediment concentration (SSC) in Sydney Harbour. Dynamic suspension events induced by shipping, e.g. mobile suspension clouds caused by bottom stirring, were observed in real-time as images on a PC screen. ABS instruments have only been developed in the last decade and are not in widespread use. They have the advantage of being able to rapidly measure high resolution temporal and spatial SSC profiles remotely and non-intrusively, and thereby to image suspension processes. Time series of raw backscatter profiles can be obtained and displayed in real-time at the temporal and spatial scales of suspension processes, making ABS devices far superior to traditional point sampling methods using water bottles and optical instrumentation. Acoustic theory for this class of instrument is briefly outlined, and simple modelling is carried out to provide background information and to examine possible calibration methods. Of particular interest is the development of routine methods to calibrate ABS instruments in the field.

## 1. INTRODUCTION

Measurements of suspended sediment concentration (SSC) profiles in aquatic environments are used for diverse purposes e.g. examination of turbidity or water clarity, pollution studies, underwater visibility, sediment transport rates, and knowledge of the dynamics affecting turbidity e.g. wave processes. Profiles are usually obtained by point sampling, using water samplers or optical instrumentation, over time and space scales much greater than dynamic suspension processes ([3] discuss further details). In the last decade acoustic backscatter (ABS) instruments have been developed e.g. [4-7, 12-14] which are able to remotely monitor suspension events at the time and space scales of suspension events without affecting the processes. The ABS instruments infer near instantaneous undisturbed SSC profiles at high temporal (0.1-1 s) and spatial (1-10 cm) resolutions by emitting bursts of MHz frequency pulses, and recording the backscatter response from the suspended material in the water column as a function of range from the transducer. After allowance for transmission losses, and by making some simple assumptions about suspended sediment properties, the backscatter can be directly related to SSC.

In this paper we discuss measurements and calibration of SSC backscatter profiles taken in Sydney Harbour (Fig 1) using an Acoustic Suspended Sediment Monitor (ASSM) developed at Shanghai Acoustics Laboratory (see [14, 3] for a brief description of the instrument). The ASSM has previously been used to examine cohesive suspension profiles in the highly turbid waters of the Chang-jiang (Yangtze) estuary off Shanghai [10, 11]. Suspension profiles and dynamic suspension events in Sydney Harbour were monitored at 0.5 and 1.5 MHz. Only 0.5 MHz data are

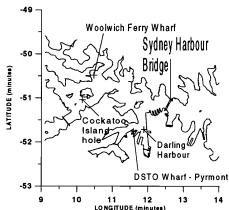


Fig 1. Locations in Sydney Harbour where an 0.5 MHz Acoustic Suspended Sediment Monitor (ASSM) and infrared wavelength nephelometer were deployed on 22 and 23 October 1997.

discussed. Independent low resolution inferences of turbidity profiles from nephelometer point measurements were used as proxy SSC calibration data. Actual measurements of SSC, which entails collection of water samples, then filtering, drying, and weighing to extract the suspended material, were not made. Modelling of backscatter profiles was carried out, based on theory provided in [13], to provide background information, to compare two calibration methods for the ASSM, and to develop calibration methods which could be applied routinely in the field. Calibration is presently performed after laboratory determinations of SSC have been obtained from water samples.

Although a specific ASSM is used, the modelling and applications are general to this class of instrument, and to the problem of inferring properties of particles suspended in a medium by means of acoustic backscatter measurements. The methods employed are not new, and no new theory is presented, but the general comparison of calibration methods, and the application of a calibration method which can be used in the field independent of laboratory measurements, should be of general interest. The paper complements an introduction to use of acoustic backscatter instrumentation to infer SSC presented by [3].

## 2. THEORY

To infer absolute values of SSC, acoustic backscatter measurements must be compensated for non-linear effects of spreading and absorption by water and suspended sediment, and a system constant incorporating the *in situ* suspended particle backscatter function must be determined. The backscatter processes may be described by single scattering theory [13]. Negligible grain shielding and negligible multiple scattering are assumed, with allowance for near and far-field transducer beam patterns, spreading, and absorption due to water and the suspended sediment itself. Absorption by suspended sediment is assumed to be proportional to SSC, a simple assumption which gives good results [13]. The attenuation constant for a particular sediment particle size may be calculated from formulae provided by [9], and absorption due to water may be calculated from temperature and salinity measurements [2].

If backscatter were sensitive to particle volume, then for constant particle density, changes in size distribution during measurements would not affect inferences of suspended sediment concentration [5]. However, in the Rayleigh region ( $k_s a \ll 1$ , where  $k_s$  is acoustic wave number and  $a$  is particle diameter), the size, shape, and density of irregularly shaped particles chiefly determine the backscatter, according to [9] and [8]. To overcome this it is commonly assumed the particle size distribution and particle backscatter function at a site are invariant during the measurements, and that only the total concentration varies at any depth in the column, a necessary but weak link in the calibration [5]. If calibration data show that size distribution does vary through the column in some deterministic manner, there is no reason to retain these two restrictions, and [4] used "calibration procedures (which) can accommodate variation of particle size with depth", but the assumptions of [5] will be used initially. The backscattered pressure or voltage signals received by the transducer from scatterers in a particular range bin are treated as incoherent [12], allowing them to be squared and summed without phase considerations. With the stated assumptions, backscatter from a particular range is linearly proportional only to concentration, and changes in raw backscatter at a particular range reflect changes in concentration. Under the assumptions, a twofold change in particle size in the Rayleigh region could cause a concentration overestimation of a factor of eight for irregularly sized particles [5]. However such large disagreements are not reported e.g. [5] quote factors of 2 to 3 for earlier work by others, and [13] and [3] found errors

around 20%. Concentration estimates could also be in error if the relative concentrations of small and large particles vary [6]. For  $k_s a \sim 1$  to 2, [6] and [8] found indications that acoustic backscatter is proportional to particle volume, thus the assumption of invariant size distribution may not be overly limiting for all particle sizes. Modelling in section 6 supports this view if size distribution does not change greatly e.g. from mud to sand size.

The backscatter equation may be written (after [5], [7] and principally [13]):

$$M(r) = V^2 (r)^2 \psi^2(r) \left[ \int_0^r \frac{1}{w(r)} \right] \left[ \int_0^r 4\alpha_w(r') dr' + \int_0^r 4\alpha_s M(r') dr' \right] \quad (1)$$

where  $k$  = a scaling factor which is a function of instrument response and of acoustic backscatter strength of the suspended sediment (the latter is assumed constant at a particular site to simplify the problem as mentioned previously);

$r$  = one way range from transducer to scatterer (m);

$c(r)$  = sound-speed at range  $r$  (ms<sup>-1</sup>);

$M(r)$  = particle mass concentration per unit volume at range  $r$  (kgm<sup>-3</sup>);

$V(r)$  = transducer response (volts) to measured backscatter pressure from range  $r$ ;

$\alpha_s$  = attenuation for unit sediment concentration (m<sup>2</sup> kg<sup>-1</sup>);

$\alpha_w$  = attenuation due to water (m<sup>-1</sup>) (The integrals allow  $\alpha_w$  and  $\alpha_s$  to vary through the water column);

$\tau$  = pulse length (s);

$\psi(r)$  = a function to account for different beam patterns in the near and far-fields, and to allow for departures from the theoretical  $1/r$  dependency in the nearfield [13].  $\psi(r) = 1$  in far-field for  $r > \epsilon r_n$  (farfield), and  $\psi(r) = (2 + (\epsilon r_n / r)) / 3$  for  $r > \epsilon r_n$  (nearfield), where  $r_n = \pi a^2 / \lambda$ , with  $a$ , the transducer radius and  $\lambda$  the acoustic wavelength. [13] chose  $\epsilon = 2$  for this definition of  $r_n$ , leading to the same definition as [5]. The 0.5 MHz ASSM has an external diameter of 18 cm, but actual transducer diameter is unknown, and was taken as 17 cm, giving  $r_n$  of 7.5 m.

Equation (1) has the same form in the near and far-fields if a cylindrical beam is assumed in the near-field and a directional beam (of constant beam angle) is assumed in the far-field. The transition region is not necessarily well defined by the expression. The expression is not in a closed form, since the required unknown  $M(r)$  occurs on both sides of the equation.  $M(r)$  may be solved for by iteration methods [15] or by direct solution [16]. For the direct solution the length of the first range interval must be chosen so the average SSC in the interval is non-zero, and the direct solution is sensitive to errors in this initial SSC value. The direct solution will not be used in this paper, but it is orders of magnitude faster than iteration, and with careful implementation this speed advantage should make it superior to iteration methods for real-time applications.

### 3. THE ASSM

Details of the ASSM may be found in [14] and [3]. In operation the downward looking 0.5 MHz ASSM is suspended about 2 m below the surface to avoid the effects of wave induced air bubbles, and may be raised and lowered if necessary to observe suspension processes. Trains of ten 40µsec pulses are transmitted, the return is time gated, and raw backscatter profiles are obtained and displayed. Beamwidth is 1.5°. To reduce variability in the Rayleigh distributed backscatter from a particular range bin, backscatter values are averages for the ten pulses. Range bins of 5 or 10 cm are used for the 0.5 MHz ASSM (with 2 cm for 1.5 MHz). The ASSM is driven by a PC, and raw backscatter profiles are displayed in real-time on the PC screen as a series of color-coded vertical bars, thus providing an image of suspension processes. Data may be obtained continuously for 15 minute bursts of about 900 profiles. Ranges of 2.2, 11, or 22 m may be selected during a deployment, and different output power selected to suit turbidity conditions. SSC range is 0.1 to 5-10  $\text{kg m}^{-3}$  (0.1  $\text{kg m}^{-3}$  is 100  $\text{mg L}^{-1}$ ). Raw data can be compensated for spherical spreading immediately after being obtained. Calibrated data are obtained in post processing by comparison against SSC determined from water samples, using software supplied with the ASSM in a "compensation method" approach discussed later.

Because of spreading losses, and attenuation by water and suspended sediment, raw backscatter values are a nonlinear function of range. Before data have been compensated for losses they must be interpreted with some care e.g. a uniform backscatter profile in the raw display indicates concentrations increasing with range. The advantage of the raw data display is that suspension processes can be observed in real-time. Increased processing speed opens the possibility of near real-time calibration from field measurements, and aspects necessary to achieve this are examined in this paper.

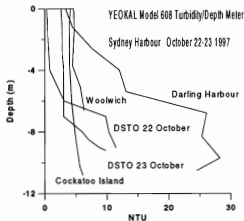


Fig 2. Nephelometer turbidity profiles for the sites of Fig 1. NTU = Nephelometric Turbidity Units. For the NTU range shown, 1 NTU is expected to indicate 1 to 2  $\text{mg L}^{-1}$ .

### 4. CALIBRATION DATA

#### 4.1 Nephelometer Data

A Yeokal model 608 Turbidity/Depth Meter (a nephelometer) was used to infer point measurements of SSC for use as calibration data for the ASSM (Fig 2). Brief comparisons of acoustic and optical turbidity instrumentation may be found in [3] and [7]. The nephelometer detects light from an 850 nm infra-red source scattered at 90° by suspended particles, and is lowered on a cable and held at particular depths until measurements stabilise, which takes several seconds. Data are reported as Nephelometric Turbidity Units (NTU). Optical sensors are subject to fouling by material in the water, the measurement is intrusive, and gives discrete points in slow time compared to the ASSM. The nephelometer is factory calibrated against a Formazin suspension, which has an unknown relation to optical backscatter response of *in situ* suspended sediment. However nephelometer output is usually linearly related to SSC, so reasonable profile shapes can be immediately available. Ideally the nephelometer should be calibrated against SSC obtained from water samples taken at the investigation site. There are potential difficulties with use of nephelometer data to calibrate ABS instruments, since nephelometers are sensitive to smaller particles, and ABS to larger. Nevertheless the real-time indications of average SSC at particular depths available from nephelometry could possibly be used to make a field calibration of the ASSM, one of the possibilities examined. Neither nephelometer nor ASSM provide estimates of suspended particle diameter, and for modelling we have assumed this from bottom type, which is soft mud. Data for nephelometer output as a function of concentration and particle size shown in [1] can be broadly interpreted as showing that for mud sizes the measured NTU approximate  $\text{mg L}^{-1}$  within a factor of 1 to 2. This indicates maximum SSC seen by the nephelometer at any site of 25 to 50  $\text{mg L}^{-1}$  in Darling Harbour, whereas the nominal minimum ASSM capability of 100  $\text{mg L}^{-1}$  is one quarter to one-half of these values. For the observed conditions the ASSM was operating below its nominal range, but some useful data were obtained which illustrate advantages and disadvantages of acoustic methods for measuring SSC.

#### 4.2 Temperature and Salinity

Measurements of temperature and salinity profiles with a Yeokal Submersible Data Logger (SDL) yielded only a few near surface values of 18.2°C and salinity of 35. To calculate acoustic absorption due to water, homogenous temperature and salinity conditions were assumed. The harbour experiences tidal stirring and no recent rainfall had occurred, so high stratification was not expected. For 0.5 MHz the formulae of [2] give absorption differences over a 20 m path between 15° and 19°C at salinity 35 of only 0.025 dB. An SDL profile taken off Pyrmont Wharf (Fig 1) four days later showed a surface to bottom temperature difference of about 2.7°C over 10 m. Applying this profile made very little difference (less than 0.025 dB) compared to using homogenous conditions.

## 5. COMPENSATION METHOD OF CALIBRATION

In software supplied with the ASSM a modified form of the backscatter equation is used to invert the backscatter profile [3]:

$$M(r) = KV^2(r)r^{-n(r)} \exp(4\alpha(r)r) \quad (2)$$

where  $\alpha(r) = \underline{\alpha}_c(r) + \underline{\alpha}_s(r)$ ,  $\underline{\alpha}_c = \zeta M(r)$ ,  $\zeta$  is the attenuation coefficient for unit concentration, and underlining specifies a column average from the transducer to range  $r$ .  $K$  is a scaling factor related to  $k$  of equation (1) as  $K = (1/\zeta c(r)) (1/k)$ .

The exponent  $n(r)$  is 1 in the near-field and 2 in the farfield to account for cylindrical and spherical spreading respectively, and varies between these limits in the transition range in an unknown manner.  $K$  and  $\zeta$  are assumed constant at each site, as detailed in section 2, and must be determined in post-processing from actual SSC calibration data sampled at each site. For each range  $r$  to a calibration point,  $\underline{\alpha}_c(r) = \zeta r / (M_{cal}(r') dr')$ , where  $M_{cal}(r')$  are calibration data, and the trapezoidal rule can be used to evaluate the integral. At calibration points in the near and far-fields,  $r^{n(r)}$  is known, and  $K$  and  $\zeta$  are the only unknowns if  $\underline{\alpha}_c(r)$  is calculated from temperature and salinity measurements, (and the backscatter function subsumed in  $K$  is assumed constant).  $\zeta$  can be calculated from a measured particle size distribution using the formulae of [9], and determinations of  $K$  can be made. Exponent  $n$  is then altered by trial and error to obtain a smooth compensation curve fitting calibration points in the transition region, a practical approach to the unknown form of  $r^{n(r)}$  there. A compensation curve  $f(r)$  is then formed to convert  $V^2(r)$  to  $M(r)$ , where  $M(r) = f(r)V^2(r)$  and  $f(r) = K r^{n(r)} \exp(4\alpha(r)r)$ . The compensation curve is applied to all profiles in a burst. The method can only provide compensation to the deepest calibration point. Since absorption is not recalculated for each profile, the compensation curve method provides considerable saving in post processing, at the possible expense of accuracy under non-static turbidity conditions. By assuming statistical stationarity, ensemble averaging can then be used to improve signal to noise ratio, with the facility provided for user selectable time-depth windowing. The procedure produces concentrations with about 20% accuracy [3]. Apparent motion of the bottom caused by sensor movements is small under usual conditions, and is not allowed for.

## 6. MODELLING

A FORTRAN computer programme was written to model backscatter based on equation (1). In section 6.1 general modelling is used to examine the compensation method of calibration; in section 6.2 an iterative calibration technique working from the surface downwards is trialled to obtain individual calibration for each profile; in section 6.3 an iterative method is trialled to obtain system constant  $k$ . For the modelling, the *in situ* backscatter function at a particular range is taken to be linearly proportional only to concentration, rather than also to shape and size distributions. As discussed in section 2, this is not necessarily true, particularly for the Rayleigh region, but is not as gross an approximation as it

might seem, as the modelling is meant to apply to a particular location, and is not meant to be transferred to another location, where the backscatter function could be different, or to be applied to the same location at a later time. Under these assumptions the modelling should give a good indication of results to be expected from use of a compensation profile approach. For the modelling,  $r_s$  of 1.5 m and  $t$  of 2 were used with a range of 10 m. The value of  $r_s$  is much smaller than for the ASSM, resulting in increased spherical spreading, providing a more general test of the calibration techniques and associated computation errors.

### 6.1 Compensation Calibration Method

Principal results of general modelling for 0.5 MHz were as follows: (i) for particle sizes in the silt range 5 to 8  $\phi$ , (where  $\phi = -\log_{10}[\text{particle diameter in mm}]$  is a logarithmic scale),  $\alpha_c$  is small, from formulae of [9], and most absorption is due to water, even for relatively high SSC. (The division from mud to sand size is at 62  $\mu\text{m}$  or 4  $\phi$ ). A compensation curve, formed from practically any shape or value profile of SSC for any  $\phi$  value between 5 to 8, functions well to calibrate a wide range of test profile SSCs and shapes in this  $\phi$  range, regardless of the exact  $\phi$  value. Even the compensation profile for water alone will suffice. This means the compensation method should work well for this  $\phi$  range in dynamic situations even though SSC changes greatly at a particular depth. (ii) Applying a compensation obtained from a constant value SSC profile, which laboratory calibrations typically provide, for values of  $\phi$  greater than 5 (smaller particle diameter) to  $\phi$  values of 4 or less (larger particles) does not always give correct results for lower measured SSC values, because increased particle absorption and non-linearity with range cause the exponentiation of equation (2) to dominate the inversion. For example spurious subsurface SSC maxima can be generated for some profile shapes which might be expected to occur naturally e.g. at the base of a mixed layer of constant concentration overlying a boundary layer with concentrations increasing towards bottom. (iii) For  $\phi$  values lower than 5 (higher particle diameter) the inversion is also dominated by the exponentiation term for very high attenuation. Low backscatter returns for some profiles can be spuriously magnified by the compensation exponential to produce very high SSCs when zero SSC should be seen, because the signal does not penetrate effectively to this range. To remove such effects backscatter values below a threshold signal to noise ratio should be set to zero, and this threshold could vary with range.

Modelling further indicated that for 0.5 MHz the compensation calibration method should work well if  $\phi$  at any particular depth does not change from mud to sand size, or from one sand size to another, and if concentration at a particular depth does not vary greatly for sand sizes. Consequently the compensation method for 0.5 MHz should yield reasonable results for mud suspensions of almost any concentration, and lower concentration sand suspensions in both static and dynamic situations. No allowance was made for multiple scattering or particle shielding in modelling, effects which may become important at high concentrations.

## 6.2 Iterative Calibration Method

Using the results of section 6.1 for mud suspensions, that practically any  $\phi$  value in the mud range would be adequate to model absorption by sediment, representative  $\phi$  values were chosen to obtain attenuation constant  $\xi$ . It was then assumed that SSC had a constant (but unknown) value over the first depth bin, and SSC was inferred from test backscatter profiles by iterating the following equation at each range  $r$ , working downwards from the first range bin:

$$M_{\text{test}}(r) = V^2(r)r^2\psi^2(r)(1/\tau(r))(1/k^2) \exp\left[\sum_{r'} 4\alpha_{\text{sed}}(r')\Delta r' + \sum_{r'} 4\alpha_{\text{w}}(r')\Delta r'\right] \quad (3)$$

where terms are as in equation (1),  $\alpha_{\text{sed}}(r') = 4\xi(0.5(M(r'-\Delta r) + M_{\text{sed}}(r')))\Delta r$ , and  $\Delta r$  is the length of the current range bin. The term  $0.5(M(r'-\Delta r) + M_{\text{sed}}(r'))$  is simply the average SSC for the current range bin.  $M_{\text{sed}}(r')$  is altered until the expression is satisfied to a required tolerance. For 0.5 MHz the iteration worked successfully for very high test SSC values ( $50 \text{ kgm}^{-3}$ ) for ranges to 10 m using nominal values of  $\phi$  and  $k$ . Correct SSC values and profile shapes were returned without requiring prior knowledge of SSC magnitudes. An iterative method was used by [12] to calculate SSC and particle diameter for maximum range 1.28 m for frequencies 1, 2.5, and 5 MHz, and SSC of 0.001 to  $2 \text{ kg.m}^{-3}$ . Iterative methods are discussed by [15].

Under actual operating conditions results at high SSC could possibly be affected by multiple scattering and particle shielding, and the absorption profile for water should be well known (through temperature and salinity measurements) to ensure the particle backscatter contribution is accurately known. This latter point is emphasised by [4] for application of an iteration technique to Acoustic Doppler Current Profiler (ADCP) data in the Pearl River region of Hong Kong, where temperature and salinity gradients can be  $1^\circ\text{C}$  and 5 salinity units per metre.

## 6.3 Iterative Determination Of ASSM System Constant

Rearranging the backscatter equation (1) for system constant  $k$  gives:

$$k^2 = V^2(r)r^2\psi^2(r)(M_{\text{cal}}(r)/\tau(r)) \exp\left[\sum_{r'} 4\alpha_{\text{sed}}(r')\Delta r' + \sum_{r'} 4\alpha_{\text{w}}(r')\Delta r'\right] \quad (4)$$

where  $M_{\text{cal}}$  are the SSC calibration values, and  $\alpha_{\text{sed}}(r') = 4\xi(0.5(M_{\text{cal}}(r'-\Delta r) + M_{\text{cal}}(r')))\Delta r$  as before. For several pairs of  $M_{\text{cal}}(r)$  this expression was evaluated by iterating on  $\xi$  until the pair of  $k$  values were closest in magnitude. For test data at 0.5 MHz,  $k$  was returned with little or no error up to ranges at least 10 m. With the usual assumptions the modelling of sections 6.2 and 6.3 indicates the possibility of automatically calibrating SSC data in the field against nephelometer or other field calibration data.

## 7. ASSM MEASUREMENTS IN SYDNEY HARBOUR

### 7.1 Despiking

Some measured time series showed intermittent strong high value spikes, apparently due to bubbles and occasional

electrical interference. Strong spikes will distort simple ensemble averages. Instead smoothed profiles were formed from profile subsets as the average of the one-third lowest values at each depth, and also from medians. Medians provided better results for low numbers of profiles in a subset (Fig 3). This smoothed profile could be used directly as an averaged profile, with improved signal to noise ratio compared to individual profiles, or as a reference profile against which to despike individual profiles in the subset. Since spikes sometimes extended over several vertical depth intervals, simple replacement of spike values with reference profile values was preferred to interpolation in the vertical. Following despiking, profiles could be further smoothed to remove noise if necessary by two-point running vertical averages or other schemes.

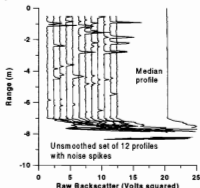


Fig 3. Example of despiking and averaging of raw acoustic backscatter profiles. The profile on the right is formed at each depth from the median of the values of the twelve profiles shown to its left. Profiles are offset from each other by 1 volt<sup>2</sup>.

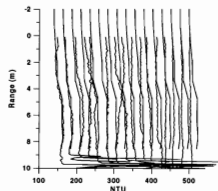


Fig 4. Calibrated ASSM data profiles calculated from medians of twelve raw profiles for Darling Harbour, overlotted on the nephelometer calibration profile. The nephelometer profile starts from the surface, which is at  $-2 \text{ m}$  relative to the ASSM transducer, and it is overlotted separately with each ASSM profile. ASSM profile shapes and values show high general correspondence with the nephelometer data at the start of the ASSM time series, when the nephelometer data were obtained. Profiles are offset by 24 NTU, with the origin at 135 NTU.

## 7.2 Calibration

The iteration procedure of 6.3 to determine  $k$  against the nephelometer data yielded  $k$  values between 250-500 for Darling Harbour, the site with highest nephelometric turbidity. SSC is then known through  $1/k^2$  to a factor of 1 to 4, a rather large range. In a sensitivity test,  $k$  of 200 and 600 gave SSC values obviously too big and too small respectively, compared to nephelometer data. The best value of  $k$  was visually determined by overplotting SSC profiles obtained with various  $k$  on the nephelometer calibration profile. There is a conundrum here in that ABS instruments are good at observing dynamic processes, but field calibration under dynamic circumstances is difficult if turbidity changes markedly at any depth during measurements, as it is then difficult to relate ABS and calibration data in both time and space. A  $k$  of 400 gave good agreement with Darling Harbour nephelometer profile values and shapes at the start of the measurements, when the nephelometer data were taken (Fig 4), which is as good a result as can be expected, since turbidity conditions were changing during the nephelometer measurements. The point of note is that after a value is determined for  $k$ , then profile shapes and values returned by the iterative methods arise through the modelled physics. No prior assumptions are made about SSC profile shapes or values, but good agreements were found against the Darling Harbour nephelometer data. The harbour results mean correct functioning for the ASSM has apparently been established through physical theory and independent measurements. There is no real reason not to have  $k$  as a function of depth, to account for changing particle properties or other conditions through the column (including beam pattern if necessary), and the iterative methods can indicate if this is necessary, but a fixed  $k$  was sufficient. A fixed  $k$  removes some of the empiricism in the methods, and is physically pleasing, as it should indicate the assumption of near constant size distribution was not violated. Although the iterative methods seemed to work satisfactorily, some inadvertent experiments in changing the near-field parameter  $rn$  from the nominal value of 7.5 m to a value as low as 1.5 m showed that  $k$  values could be found for the Darling Harbour data which gave quite reasonable results, so caution is warranted. The Darling Harbour  $k$  value was used to calibrate data at all sites, as  $k$  values at other sites could not be established.

## 7.3 Observed Suspension Profiles

At Woolwich wharf the 0.5 MHz ASSM was deployed almost immediately after a ferry had departed. An apparent suspension cloud or buoyant plume was seen in the real-time ASSM raw backscatter display, rising quickly towards the surface. The nephelometer could not operate rapidly enough to show this detail, and could not provide useful calibration data, with data taken after the observed event had ceased. ASSM data calibrated using the  $k$  for Darling Harbour (Fig 5) showed highest SSC for the survey, with SSC generally decreasing with depth and with time. At the start of the time series SSC near the transducer was over 200 NTU, falling to about 30 NTU at the end of the measurements, but the interpretation is that the high values were mainly due to buoyant rising bubbles, not sediment. Bubbles are much more

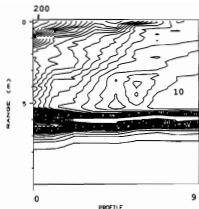


Fig 5. Woolwich Ferry Wharf 23 October. Contour plot of calibrated 0.5 MHz data (units are NTU) taken with the workboat stationary after a ferry departure. Time increases from left to right. Data are calculated from medians of twelve raw profiles. The pattern represents a rising bubble plume, possibly advecting suspended sediment. Contour clustering at 6 m range marks the bottom.

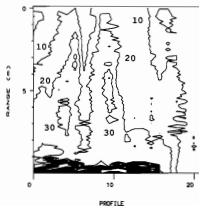


Fig 6. Darling Harbour 23 October. Contour plot of calibrated 0.5 MHz data (units are NTU) taken with the workboat drifting, calculated from medians of nine raw profiles. The pattern represents two turbid plumes at profiles 5 and 9 separated by clearer water at profile 6, caused by a tug stirring the bottom. The bottom is at 9 m range.

efficient at scattering than equivalent sized sediment, particularly at resonance [5]. As the turbulent stirring mechanism ceases, particles would be expected to fall after experiencing rises, with SSC then rising with depth and decreasing with time through the column, but this was not observed. This example illustrates the problems that bubbles can cause high frequency acoustic marine instruments. Optical instruments are similarly affected.

At Darling Harbour the opportunity was taken to drift over waters which had been disturbed by tugs assisting a ship to leave berth some minutes earlier. Bottom sediments could be seen by

eye to have been entrained into the water column. Highest nephelometer levels for the survey were seen. The ASSM showed the boat to be drifting over suspension clouds, with the depth of the top of the clouds varying along track (Fig 6), consistent with visible surface indications of patchiness in the turbidity. The nephelometer could not operate rapidly enough to show this detail, and provided only broad indications of turbidity at the start of the ASSM measurements, but this was able to provide the calibration previously described in section 7.2. Column turbidity in Figure 6 is notably higher over shallower depths, as might be expected when turbidity is caused by a bottom stirring mechanism.

Off Cockatoo Island the nephelometer showed the concentration of suspended material to be very low and increasing slowly from surface to bottom. The iterative method broadly matched nephelometer data, however the increase in concentration with depth was possibly due to noise levels being amplified by the non-linear range-squared and absorption terms. At Pyrmont the nephelometer showed a two-layer system with low turbidity visibly clear water overlying a more turbid lower column. A 50 kHz Furuno echosounder showed an intermittent scattering layer about 6 m below the surface, apparently corresponding to the gradient seen by the nephelometer. Raw acoustic backscatter values were nearly constant through the column, and it appeared only noise levels were measured, resulting in calibrated ASSM values from the iterative method increasing approximately linearly from the transducer to bottom with the correct magnitude, but without the mid-column gradient region. The nephelometer indicated SSC far below the nominal lower level of the ASSM, and the ASSM could not be expected to function, but these two examples show the importance of obtaining calibration data at each site, and of subtracting noise. The ASSM correctly showed that SSC levels were low, and this could be considered a positive result for the iteration methods and the ASSM.

## 8. DISCUSSION

Rapid high resolution measurements of dynamic suspended sediment concentration profiles were obtained in Sydney Harbour with an Acoustic Suspended Sediment Monitor (ASSM) developed by Shanghai Acoustics Laboratory. The ASSM was used while stationary and drifting, in the latter case effectively showing a cross-section of suspended sediment concentration (SSC). The nominal lower limit of SSC for the 0.5 MHz ASSM of 100 mgL<sup>-1</sup> indicates it is suited to quite turbid conditions, but suspension events were successfully observed at lower turbidity levels.

Modelling indicated a compensation method of calibration supplied in software with the ASSM should be reliable in dynamic situations for mud suspensions to very high concentrations, and lower concentration sand suspensions. The compensation technique applies a single calibration profile to all profiles in a data burst, and does not allow for absorption due to SSC to change with time through the column if SSC changes, as will happen for dynamic events. Modelling and field results indicated iterative calibration techniques could supplement or replace the compensation method, since they can calibrate the full measured profile, they can be applied to individual profiles, they can be applied semi-automatically, and they are much less empirical. If nephelometric or other estimates of SSC are available in the

field, modelling and measurement indicate that useful ASSM near real-time calibration could be obtained routinely through application of iterative methods, which appear quite robust. The ASSM appears to be a highly versatile instrument able to be used routinely in the field to observe dynamic turbidity events and suspension profiles.

## ACKNOWLEDGEMENTS

The ASSM was operated by Prof. S.Y. Zhang, L.F. Ren, and H.L. Lin of Shanghai Acoustics Laboratory, and G. Sidim of the University of New South Wales. Raw ASSM data were supplied by Dr J. Dunlop of the University of New South Wales, from whom the ASSM may be leased.

## REFERENCES

1. D&A Instruments, OBS® suspended solids & turbidity monitors. D&A Instrument Company pamphlet rev 11/91, Port Townsend, WA 98368 (1991) 4pp
2. R.E. Francois and G.R. Garrison, Sound absorption based on ocean measurements: Part 1: Pure water and magnesium sulfate contributions. *J. Geost. Soc. Am.* 72(3), 896-907 (1982)
3. L.J. Hamilton, Z. Shi and S.Y. Zhang, Acoustic Backscatter Measurements of Estuarine Suspended Cohesive Sediment Concentration Profiles. *J. Coastal Research* 14, 1213-1224 (1998)
4. J.M. Land, R. Kirby and J.B. Massey, Ch 12 Developments in the combined use of acoustic doppler current profilers and profiling salinimeters for suspended solids monitoring. In *Cohesive Sediments, Off-Nearshore and Estuarine Cohesive Sediment Transport Conference: INTERCOH '94*. Eds Burt, Parker and Watts. John Wiley & Sons (1997) pp. 187-196.
5. C. Libicki, K.W. Bedford and J.F. Lynch, The interpretation and evaluation of a 3-MHz acoustic backscatter device for measuring benthic boundary layer sediment dynamics. *J. Acoust. Soc. Am.* 85(4), 1501-1511 (1989)
6. J.F. Lynch, J.D. Irish, C.R. Sherwood and Y.C. Agrawal, Determining suspended sediment particle size information from acoustic and optical backscatter measurements. *Continental Shelf Research* 14(10/11), 1139-1165 (1994)
7. P.D. Osborne, C.E. Vincent and B. Greenwood, Measurements of suspended sand concentrations in the seashore: field intercomparison of optical and acoustic backscatter sensors. *Continental Shelf Research* 14, 159-174 (1994)
8. A.S. Schaafsma and A.E. Hay, Attenuation in suspensions of irregularly shaped sediment particles: A two-parameter equivalent spherical scatterer model. *J. Acoust. Soc. Am.* 102(3), 1485-1502 (1997)
9. J. Sheng J. and A.E. Hay, An examination of the spherical scatterer approximation in aqueous suspensions of sand. *J. Acoust. Soc. Am.* 83(2), 598-610 (1988)
10. Z. Shi, L.F. Ren and H.L. Lin, Vertical suspension profile in the Changjiang Estuary. *Marine Geology* 30, 29-37 (1996)
11. Z. Shi, L.F. Ren, S.Y. Zhang and J.Y. Chen, Acoustic imaging of cohesive sediment resuspension and re-entrainment in the Changjiang Estuary, East China Sea. *Geo-Marine Letters* 17, 162-168 (1997)
12. P.D. Thorne and P.J. Hardcastle, Acoustic measurements of suspended sediments in turbulent currents and comparison with in-situ samples. *J. Geost. Soc. Am.* 101(5), Pt 1, 2603-2614 (1997)
13. P.D. Thorne, C.E. Vincent, P.J. Hardcastle, S. Rehman and N. Pearson, Measuring suspended sediment concentration using acoustic backscatter devices. *Marine Geology* 98, 7-16 (1991)
14. S.Y. Zhang, Some progress in underwater acoustic geo-mapping technology. *Acoustics Australia* 24(2), 47-51 (1996)
15. T. H. Lee and J.M. Hanes, Direct inversion method to measure the concentration profile of suspended particles using backscattered sound. *J. Geophysical Research* 100, C2, 2649-2657.
16. E.D. Thosteson and D.M. Hanes, A simplified method for determining sediment size and concentration from multiple frequency acoustic backscatter measurements. *J. Acoust. Soc. Am.* 104(2), Pt 1, 820-830.